$[NiM_r]^{3+}$ and $3.5 \times 10^4$ $M^{-1}$ for $[Ni(tet\text{-}c)]^{3+}$. These values are very similar, as might be expected for complexes with related sterically crowded axial coordination sites. They also appear to be much larger than the $K$ value for $Cl^-$ and $Br^-$ ($K$ for $[NiM_r]^{3+} + Cl^-$, 640 $M^{-1}$). This implies that the thermodynamic stability of the iodonickel(III) complex is much greater than that of the chloronickel(III) complex. This can once again be attributed to the increased nephelauxetic effect of $I^-$ over that of $Cl^-$, resulting in a more covalent Ni-X bond. Also, for the iodide reductions, the major component to the activation energy is due to the enthalpy term. The formation of the iodo complex is dominated by a large increase in entropy, consistent with reduced solvation on charge neutralization.

**Comparison with Cu(III) and Ni(III) Peptide Complexes.** It is of interest to compare the kinetics and mechanism of reactions under consideration with those for Ni(III)[11] and Cu(III)[12] peptide complexes. As discussed in the Introduction, in the case of $Ni^{III}H_{-2}Aib_3$), the order is always second order in $[I^-]$, and there are two pathways, which are second order (major route) and first order (minor route) in [Ni(III)]. These results are explained in terms of a mechanism wherein the iodonickel(III) complex reacts either with another iodonickel(III) species or with $I^-$ to produce $I_2$ or $I_2^-$, respectively. These oxidations are thermodynamically more favorable than the oxidation of $I^-$ to $I^\bullet$. The relevant $E°$ values have been estimated[17] at 0.620 V ($2I^- \rightarrow I_2$), 1.08 V ($2I^- \rightarrow I_2^-$), and 1.40 V ($I^- \rightarrow I^\bullet$). Thus, the $Ni^{III}(H_{-2}Aib_3)$ complex, which is very axially labile,[10] has as its major route for iodide oxidation the reaction of two iodonickel(III) complexes to produce $I_2$ in a pathway with the lowest $E°$ or greatest thermodynamic ease. The minor route takes the next most thermodynamically feasible process, by oxidizing $2I^-$ to $I_2^-$.

In the case of the Cu(III) peptides,[12] the complexes are axially inert, eliminating a bimolecular reaction of two complexes. At high concentrations of $I^-$, the mechanism appears to involve the reaction of an outer-sphere complex $[Cu^{III}H_{-n}L,I^-]$ with $I^-$ to produce $I_2^-$. At lower concentrations of iodide, the most thermodynamically unfavorable pathway, involving oxidation of $I^\bullet$ to $I^-$, becomes dominant.

In the Ni(III) macrocycles under study, the complexes are fairly labile, but not as labile as Ni(III) peptide complexes,[6] so that a reaction pathway involving two $[NiLI]^{2+}$ species does not occur. However, the equilibrium constant for formation of the monoiodo complex is much larger (e.g. $3.6 \times 10^4$ $M^{-1}$ for $[NiM_r]^{3+}$ compared with $\leq 10$ $M^{-1}$ for $Ni(H_{-2}Abi_3)$). The complex decomposition rate $k_{-3}$ thus does not compete with the electron-transfer step in the case of the macrocyclic complexes, leading to a first-order, rather than a second-order, dependence on $[I^-]$ (eq 12).

**Acid Dependence.** It can be seen (Table II) that the rate of iodide oxidation by $[NiM_m]^{3+}$ increases slightly with $[H^+]$. The derived dependence leads to eq 14, with a value of 494 $M^{-2}$ $s^{-1}$

$$k_{3,obsd} = k_3 + k_{3,h}[H^+] \quad (14)$$

for $k_{3,h}$ at 21 °C. It was previously reported[9] that there was no acid dependence in the case of the reaction with $[Ni(cyclam)]^{3+}$, but this was based on only two measurements, at 0.1 and 1.0 M $H^+$ and ionic strength 1.0 M. A more detailed study of the cyclam system over the range 0.05-3.0 M $H^+$ at 3.0 M ionic strength revealed a similar linear dependence on $[H^+]$, with a third-order rate constant $k_{3,h} = 280$ $M^{-2}$ $s^{-1}$.

An increase in rate with acid concentration was seen in the reaction of $I^-$ with some of the Cu(III) peptide complexes and with $Ni(H_{-2}Aib_3)$. This was attributed to the formation of an externally protonated species in which the peptide oxygen is protonated. In the case of the Ni(III) macrocycles, however, no such outside protonation can occur, since the nitrogens are already four-coordinate. Neither is the mechanism likely to involve a protonated $I^-$ species, since the p$K$ value for HI has been estimated at -11.[28] No first-order acid dependence was observed in the $Cl^-$ and $Br^-$ substitution reactions of these Ni(III) macrocycles. The mechanism of this acid-catalyzed pathway is thus unclear at present. However, the origins of the effect may lie in the fact that although the ionic strength is maintained constant, the ionic environment changes greatly for $[H^+] = 0.05$-3.0 M.

## Conclusions

It has been shown, on the basis of spectroscopic and kinetic data, and by comparison with outer-sphere reactions via a Marcus correlation, that the oxidation of iodide ion by five Ni(III) macrocyclic complexes is inner sphere, proceeding by formation of a iodonickel(III) complex followed by reaction with another $I^-$ ion to produce $I_2^-$. The predominance of this pathway over other possible routes has been rationalized by comparison of the redox and substitution properties of these complexes with those of similar species for which the oxidation of iodide has been studied.

**Acknowledgment.** Financial support from the Natural Sciences and Engineering Research Council (Canada) is gratefully acknowledged. M.G.F. thanks the University of Victoria for a Graduate Fellowship.

**Registry No.** $[NiM_m](ClO_4)_2$, 96947-08-9; $[NiE_m](ClO_4)_2$, 96866-27-2; $[Ni(tet\text{-}c)](ClO_4)_2$, 16337-61-4; $[NiM_r](ClO_4)_2$, 96947-10-3; $I^-$, 20461-54-5.

**Supplementary Material Available:** A table of observed rate constants for iodide reduction of nickel(III) macrocyclic complexes (3 pages). Ordering information is given on any current masthead page.

(28) *The Chemists Companion*; Gordon, A. J., Ford, R. A., Eds.; Wiley: New York, 1972; p 58.

Contribution from the Department of Chemistry and Laboratory for Molecular Structure and Bonding, Texas A&M University, College Station, Texas 77843

# Crystal Structures of Two $MoOX_2L_3$ Complexes, $MoOCl_2(PMePh_2)_3$ and $MoO(NCO)_2(PEt_2Ph)_3$. Implications to Distortional Isomerism

F. Albert Cotton,* Michael P. Diebold, and Wieslaw J. Roth

*Received January 25, 1987*

The molecular structures of two $MoOX_2L_3$ complexes, green $MoOCl_2(PMePh_2)_3$ (**1**) and blue $MoO(NCO)_2(PEt_2Ph)_3$ (**2**), are reported. Compound **1** crystallizes in the triclinic space group $P\bar{1}$ with $a = 10.433$ (3) Å, $b = 18.871$ (5) Å, $c = 9.981$ (3) Å, $\alpha = 96.56$ (2)°, $\beta = 107.02$ (2)°, $\gamma = 77.83$ (2)°, $V = 1834$ (2) Å$^3$, and $Z = 2$. Compound **2** also crystallizes in space group $P\bar{1}$ with $a = 17.887$ (3) Å, $b = 17.912$ (4) Å, $c = 11.330$ (2) Å, $\alpha = 94.78$ (2)°, $\beta = 107.33$ (1)°, $\gamma = 85.39$ (2)°, $V = 3447$ (1) Å$^3$, and $Z = 4$. Most notable is the Mo=O distance in **1** (1.669 Å), which is much shorter than the Mo=O distance in green $MoOCl_2(PEt_2Ph)_3$ (1.803 Å) and comparable to that in the blue isomer of $MoOCl_2(PMe_2Ph)_3$ (1.676 Å) and in blue **2** (average 1.684 Å). Implications of this short bond distance in **1** are discussed.

## Introduction

Coordination compounds that have the same ligands and the same overall geometry but differ in specific bond lengths and angles are termed "distortional isomers". The first examples of such compounds were molecules of the type $MoOX_2L_3$, where X = halogen or pseudohalogen and L = phosphine or arsine.[1,2] Most

0020-1669/87/1326-2848$01.50/0 

of these compounds are either green or blue in color. However, two of them, $MoOCl_2(PMe_2Ph)_3$ and $MoOCl_2(PMe_3)_3$,[3] each exist as both a green and a blue isomer. Using X-ray diffraction data from $MoOCl_2(PEt_2Ph)_3$ (a green compound) and the blue isomer of $MoOCl_2(PMe_2Ph)_3$, Chatt et al. revealed that in both the blue and green complexes the ligands take on an identical cis-mer configuration about the central metal atom.[2] Several differences in specific bond lengths and angles were noted, but because the two molecules had different phosphine ligands, it was not possible to ascertain which differences in atomic dimensions were caused by distortional isomerism and which were simply caused by the different steric and electronic requirements of the ligands. Among the differences found by Chatt were shorter M=O and longer $M—Cl_{trans\text{-}to\text{-}O}$ distances in the blue complex. In blue $MoOCl_2(PMe_2Ph)_3$ the M=O distance is 1.676 Å and the $Mo—Cl_{trans\text{-}to\text{-}O}$ distance is 2.551 Å while in $MoOCl_2(PEt_2Ph)_3$ these distances are 1.803 and 2.426 Å, respectively. Haymore et al. isolated the green isomer of $MoOCl_2(PMe_2Ph)_3$ and characterized it structurally at −160 °C.[4] The Mo–O distance was long, 1.80 (2) Å, as expected, but problems with disorder prevented an accurate determination.

Distortional isomerism has since been found in other complexes of the type $MOL_5^n$, where M = Mo or W. Wieghardt et al. have observed distortional isomers of $MoO(CN)_4(H_2O)^{2-}$ and $MoO(CN)_5^{3-}$.[5,6] They have also isolated and structurally characterized distortional isomers of $WOCl_2L'^{+}$, where L' is the cyclic tridentate ligand 1,4,7-trimethyl-1,4,7-triazacyclononane.[6] In all these cases the properties of the two isomers are similar in almost every respect (e.g. $^1H$ NMR,[3] $^{95}Mo$ NMR[7]) except color and the M=O stretching frequency. Always one isomer was blue and the other green, and, when measured, the blue isomer always had a slightly higher energy $\nu$(M–O) than the green. Wieghardt found that the only significant structural difference between the green and blue isomers of $WOCl_2L'^{+}$ were the lengths of the W=O and $W—N_{trans\text{-}to\text{-}O}$ bonds.[6] In the blue complex these lengths are 1.72 and 2.37 Å, respectively, while in the green isomer they are 1.89 and 2.32 Å. These types of differences, shorter M=O and longer $M—L_{trans\text{-}to\text{-}O}$ distances in the blue complex, are the same as Chatt found between the blue isomer of $MoOCl_2(PMe_2Ph)_3$ and green $MoOCl_2(PEt_2Ph)_3$. Lincoln and Koch have recently reported two isomers of $[HB(pz)_3MoOCl]_2O$.[8] The two compounds were geometric isomers (the two monomeric units had different orientations with respect to one another), and in addition, the $Mo–O_t$ and $Mo–N_{trans\text{-}to\text{-}O(t)}$ distances were significantly different. Lincoln and Koch attributed these differences in distances to distortional isomerism. Unfortunately, interpretation of the differences in spectroscopic properties in terms of distortional isomerism is in this case complicated by the geometric isomerism. Distortional isomerism has also been seen in $ReNX_2L_3$ (X = Cl; L = $PMe_2Ph$, $PEt_2Ph$) compounds.[9]

We now wish to report the structures of two more $MoOX_2L_3$ complexes, namely green $MoOCl_2(PMePh_2)_3$ and blue $MoO(NCO)_2(PEt_2Ph)_3$.

## Experimental Section

The high-yield syntheses of $MoOCl_2(PMePh_2)_3$ and $MoO(NCO)_2(PEt_2Ph)_3$ have previously been reported.[1] In each case a well-shaped prismatic crystal was epoxied to the tip of a glass fiber and mounted on an automated diffractometer. The unit cell determinations and collections of intensity data were carried out by following procedures routine to this laboratory and described elsewhere in detail.[10] Specific details of the data collection for both compounds are summarized in Table I. Data were corrected for Lorentz and polarization effects, and empirical absorption corrections based on azimuthal ($\psi$) scans of nine reflections with Eularian angle $\chi$ near 90° were made.

Compound **1** was treated in space group $P1$ from the onset because of initial difficulties in refining the structure in space group $P\bar{1}$. The Mo positions were determined from a Patterson map, and the inner coordination spheres were located through alternating least-squares refinements and difference Fourier maps. At this point the structure was transformed to space group $P\bar{1}$ and this assignment was confirmed by successful refinement. The remaining non-hydrogen atoms were located in a difference Fourier map. All atoms were then made anisotropic and the structure refined to convergence. The final difference Fourier map revealed two relatively large peaks (1.2 and 0.9 e/Å$^3$), but these were both

**Table I.** Crystal Data for **1** and **2**

| | | |
|---|---|---|
| formula | $MoCl_2P_3OC_{39}H_{39}$ | $MoP_3O_3N_2C_{32}H_{45}$ |
| fw | 783.51 | 694.59 |
| space group | $P\bar{1}$ | $P\bar{1}$ |
| $a$, Å | 10.433 (3) | 17.887 (3) |
| $b$, Å | 18.871 (5) | 17.912 (4) |
| $c$, Å | 9.981 (3) | 11.330 (2) |
| $\alpha$, deg | 96.56 (2) | 94.78 (2) |
| $\beta$, deg | 107.02 (2) | 107.33 (1) |
| $\gamma$, deg | 77.83 (2) | 85.39 (2) |
| $V$, Å$^3$ | 1834 (2) | 3447 (1) |
| $Z$ | 2 | 4 |
| $d_{calcd}$, g/cm$^3$ | 1.425 | 1.338 |
| cryst size, mm | 0.3 × 0.3 × 0.2 | 0.1 × 0.3 × 0.3 |
| $\mu$(Mo K$\alpha$), cm$^{-1}$ | 6.565 | 5.394 |
| data collcn instrument | CAD-4 | Syntex P$\bar{1}$ |
| radiation (monochromated in incident beam) | Mo K$_\alpha$ ($\lambda_\alpha$ = 0.71073 Å) | Mo K$\alpha$ ($\lambda_\alpha$ = 0.71073 Å) |
| orientation reflcns: no.; range (2$\theta$), deg | 25; 15.0 < 2$\theta$ < 36.0 | 15; 20.0 < 2$\theta$ < 31.0 |
| temp, °C | 20 | 6 |
| scan method | $\theta$–2$\theta$ | $\theta$–2$\theta$ |
| data collcn range (2$\theta$), deg | 5.0 < 2$\theta$ < 50.0 | 4.0 < 2$\theta$ < 45.0 |
| no. of unique data, tot. | 5125 | 3995 |
| no. of data with $F_o^2 > 3\sigma(F_o^2)$ | 3936 | 3265 |
| no. of param refined | 415 | 439 |
| transmissn factors: max; min | 0.9978; 0.7621 | 0.9997; 0.8964 |
| $R^a$ | 0.0544 | 0.0590 |
| $R_w^b$ | 0.0670 | 0.0743 |
| quality-of-fit indicator$^c$ | 1.6065 | 1.492 |
| largest shift/esd, final cycle | 0.03 | 0.24 |
| largest peak, e/Å$^3$ | 1.20 | 0.563 |

$^a R = \sum||F_o| - |F_c||/\sum|F_o|$. $^b R_w = [\sum w(|F_o| - |F_c|)^2/\sum w|F_o|^2]^{1/2}$; $w = 1/\sigma^2(|F_o|)$. $^c$Quality-of-fit = $[\sum w(|F_o| - |F_c|)^2/(N_{observns} - N_{params})]^{1/2}$.

**Table II.** Final Atomic Positional and Isotropic Equivalent Displacement Parameters for $MoOCl_2(PMePh_2)_3$[a]

| atom | $x$ | $y$ | $z$ | $B$,[b] Å$^2$ |
|---|---|---|---|---|
| Mo(1) | 0.31368 (6) | 0.24644 (3) | 0.14250 (6) | 2.34 (1) |
| Cl(1) | 0.1939 (2) | 0.3414 (1) | 0.2851 (2) | 3.57 (4) |
| Cl(2) | 0.5132 (2) | 0.2211 (1) | 0.3491 (2) | 3.68 (5) |
| P(1) | 0.0908 (2) | 0.2778 (1) | −0.0519 (2) | 2.62 (4) |
| P(2) | 0.2297 (2) | 0.1576 (1) | 0.2598 (2) | 2.92 (4) |
| P(3) | 0.4151 (2) | 0.3539 (1) | 0.1065 (2) | 2.81 (4) |
| O | 0.3714 (5) | 0.1896 (3) | 0.0232 (5) | 3.5 (1) |

[a] Carbon atom positions are given as supplementary material. [b] Values for anisotropically atoms are given in the form of the isotropic equivalent thermal parameter defined as $^4/_3[a^2\beta_{11} + b^2\beta_{22} + c^2\beta_{33} + ab(\cos\gamma)\beta_{12} + ac(\cos\beta)\beta_{13} + bc(\cos\alpha)\beta_{23}]$.

(1) Butcher, A. V.; Chatt, J. *J. Chem. Soc. A* **1970**, 2652.
(2) (a) Chatt, J.; Muir, K. W.; Manojlovic-Muir, L. *J. Chem. Soc., Chem. Commun.* **1971**, 147. (b) Manojlovic-Muir, L. *J. Chem. Soc. A* **1971**, 2796. (c) Manojlovic-Muir, L.; Muir, K. W. *J. Chem. Soc., Dalton Trans.* **1972**, 686.
(3) Carmona, E.; Galindo, A.; Sanchez, L.; Nielson, A.; Wilkinson, G. *Polyhedron* **1984**, *3*, 347.
(4) Haymore, B. L.; Goddard, W. A., III; Alison, J. C. *Proc. Int. Conf. Coord. Chem., 23rd* **1984**, 535.
(5) Wieghardt, K.; Backes-Dahmann, G.; Holzbach, W.; Swiridoff, W. J.; Weiss, J. *Z. Anorg. Allg. Chem.* **1983**, *44*, 499.
(6) (a) Wieghardt, K.; Backes-Dahmann, G.; Nuber, B.; Weiss, J. *Angew. Chem., Int. Ed. Engl.* **1985**, *24*, 777. (b) Backes-Dahmann, G.; Wieghardt, K. *Inorg. Chem.* **1985**, *24*, 4049.
(7) Young, C. G.; Enemark, J. H. *Inorg. Chem.* **1985**, *24*, 4416.
(8) Lincoln, S.; Koch, S. A. *Inorg. Chem.* **1985**, *25*, 1594.
(9) Dilworth, J. R.; Dahlstrom, P. L.; Hyde, J. R.; Zubieta, J. *Inorg. Chim. Acta* **1983**, *71*, 21.
(10) (a) Bino, A.; Cotton, F. A.; Fanwick, P. E. *Inorg. Chem.* **1979**, *18*, 3558. (b) Cotton, F. A.; Frenz, B. A.; Deganello, G.; Shaver, A. *J. Organomet. Chem.* **1973**, *50*, 227.

**Table III.** Final Atomic Positional and Isotropic Equivalent Displacement Parameters for $MoO(NCO)_2(PEt_2Ph)_3$[a]

| atom | x | y | z | B,[b] Å² |
|---|---|---|---|---|
| Mo | 0.31733 (7) | 0.29181 (7) | 0.0890 (1) | 3.16 (3) |
| P(1) | 0.4348 (2) | 0.3602 (2) | 0.0812 (4) | 3.6 (1) |
| P(2) | 0.3747 (2) | 0.1631 (2) | 0.0354 (4) | 3.4 (1) |
| P(3) | 0.2412 (2) | 0.4041 (2) | 0.1656 (4) | 3.7 (1) |
| O(1) | 0.2735 (6) | 0.3060 (5) | −0.0611 (9) | 4.3 (3) |
| N(2) | 0.3913 (7) | 0.2806 (7) | 0.279 (1) | 4.3 (3) |
| C(2) | 0.4248 (9) | 0.264 (1) | 0.373 (1) | 4.9 (4) |
| O(2) | 0.4634 (8) | 0.2419 (8) | 0.474 (1) | 9.5 (5) |
| N(3) | 0.2361 (6) | 0.2305 (7) | 0.136 (1) | 4.5 (3) |
| C(3) | 0.1786 (9) | 0.2100 (8) | 0.135 (1) | 4.2 (4) |
| O(3) | 0.1140 (6) | 0.1894 (6) | 0.134 (1) | 6.9 (3) |
| Mo′ | 0.12344 (7) | 0.81686 (7) | 0.5045 (1) | 3.17 (3) |
| P(1)′ | 0.0443 (2) | 0.7556 (2) | 0.3020 (4) | 3.4 (1) |
| P(2)′ | 0.0194 (2) | 0.8033 (2) | 0.6133 (4) | 3.6 (1) |
| P(3)′ | 0.2455 (2) | 0.8386 (2) | 0.4384 (4) | 3.6 (1) |
| O(1)′ | 0.0871 (5) | 0.9033 (5) | 0.4593 (9) | 4.1 (3) |
| N(2)′ | 0.1633 (7) | 0.6988 (6) | 0.519 (1) | 4.7 (4) |
| C(2)′ | 0.1871 (9) | 0.6376 (9) | 0.535 (2) | 5.3 (5) |
| O(2)′ | 0.2112 (9) | 0.5732 (7) | 0.546 (2) | 11.6 (6) |
| N(3)′ | 0.1982 (7) | 0.8318 (7) | 0.685 (1) | 4.8 (4) |
| C(3)′ | 0.246 (1) | 0.8221 (9) | 0.774 (1) | 5.0 (4) |
| O(3)′ | 0.2950 (9) | 0.8125 (9) | 0.873 (1) | 10.7 (5) |

[a] Phenyl carbon atom positions are reported as supplementary material. [b] Values for anisotropically refined atoms are given in the form of the isotropic equivalent thermal parameter defined as $^4/_3[a^2\beta_{11} + b^2\beta_{22} + c^2\beta_{33} + ab(\cos\gamma)\beta_{12} + ac(\cos\beta)\beta_{13} + bc(\cos\alpha)\beta_{23}]$.

located near the molybdenum atom and were considered artifacts of series termination. Final atomic positional and isotropic equivalent displacement parameters for **1** are listed in Table II.

On the basis of the large cell volume, two independent molecules of $MoO(NCO)_2(PEt_2Ph)_3$ were assumed in the asymmetric unit. The positions of the two metal atoms were determined from a three-dimensional Patterson map. The remaining non-hydrogen atoms were located through a series of least-squares refinements and difference Fourier maps. All atoms except the carbon atoms on the phosphine ligands were made anisotropic, and the structure was refined to convergence. Final atomic positional parameters and isotropic equivalent displacement parameters are given in Table III. A complete listing of anisotropic displacement parameters and observed and calculated structure factors for both compounds is available as supplementary material.

## Results

Selected bond distances and angles for $MoOCl_2(PMePh_2)_3$ and $MoO(NCO)_2(PEt_2Ph)_3$, as well as the previously reported $MoOCl_2(PMe_2Ph)_3$[2b] and $MoOCl_2(PEt_2Ph)_3$[2c] complexes, are

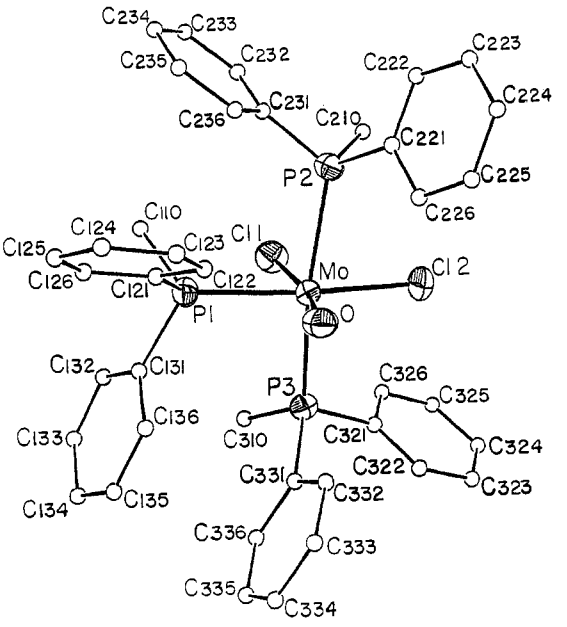


**Figure 1.** ORTEP view of $MoOCl_2(PMePh_2)_3$ (**1**). Carbon atoms are shown with arbitrarily small displacement parameters for the sake of clarity.

presented in Table IV. A complete listing of bond distances and angles for **1** and **2** is available as supplementary material. An ORTEP drawing of **1** is shown in Figure 1, and ORTEP view of both independent monomers of **2** are shown in Figure 2.

The crystal structure of $MoOCl_2(PMePh_2)_3$ consists of discrete monomeric units. As in $MoOCl_2(PMe_2Ph)_3$ and $MoOCl_2(PEt_2Ph)_3$, the ligands adopt an octahedral cis-mer configuration about a central molybdenum atom. The most significant angular deviation from octahedral symmetry is the bending of the P(2) and P(3) atoms away from P(1), resulting in the P(2)–Mo–P(3) angle being only 161°. This bending can be attributed to steric factors, as it relieves intramolecular repulsions among the bulky phosphine ligands. The organic constituents on each of the methyldiphenylphosphine ligands have the same relative orientation with respect to the plane made up by the three phosphorous atoms. Specifically, on each phosphine the centroid of one phenyl ring lies in the plane of the phosphorous atoms, and that phenyl group is roughly perpendicular to this plane. The other phenyl ring lies

**Table IV.** List of Important Bond Distances (Å) and Angles (deg) for Structurally Characterized $MoOX_2L_3$ Complexes[a]

| | 1[b] | 2a[b] | 2b[b] | $MoOCl_2(PMe_2Ph)_3$[c] | $MoOCl_2(PEt_2Ph)_3$[c] |
|---|---|---|---|---|---|
| | | | (A) Distances (Å) | | |
| Mo–O | 1.667 (4) | 1.678 (8) | 1.690 (8) | 1.676 (7) | 1.803 (11) |
| Mo–X(1) | 2.509 (2) | 2.18 (1) | 2.18 (1) | 2.551 (3) | 2.426 (6) |
| Mo–X(2) | 2.466 (2) | 2.10 (1) | 2.09 (1) | 2.464 (3) | 2.479 (5) |
| Mo–P(1) | 2.555 (2) | 2.542 (4) | 2.524 (4) | 2.500 (3) | 2.521 (5) |
| Mo–P(2) | 2.570 (2) | 2.548 (4) | 2.555 (4) | 2.541 (3) | 2.582 (6) |
| Mo–P(3) | 2.577 (2) | 2.575 (4) | 2.577 (4) | 2.558 (3) | 2.556 (6) |
| | | | (B) Angles (deg) | | |
| O–Mo–X(1) | 169.8 (2) | 170.5 (4) | 167.3 (4) | 168.8 (3) | 170.0 (4) |
| O–Mo–X(2) | 99.5 (2) | 102.9 (4) | 106.5 (5) | 105.7 (3) | 98.8 (4) |
| O–Mo–P(1) | 86.5 (2) | 90.0 (3) | 91.8 (3) | 91.9 (3) | 93.4 (4) |
| O–Mo–P(2) | 99.9 (1) | 91.7 (3) | 93.1 (3) | 91.7 (3) | 89.7 (4) |
| O–Mo–P(3) | 95.7 (1) | 93.6 (3) | 88.4 (3) | 91.2 (3) | 89.6 (4) |
| X(1)–Mo–X(2) | 90.52 (6) | 86.5 (5) | 85.3 (5) | 85.5 (1) | 86.2 (2) |
| X(1)–Mo–P(1) | 83.60 (5) | 80.6 (3) | 76.6 (3) | 85.5 (1) | 86.2 (2) |
| X(1)–Mo–P(2) | 83.81 (5) | 87.6 (3) | 92.7 (3) | 89.4 (1) | 90.8 (2) |
| X(1)–Mo–P(3) | 82.58 (5) | 89.2 (3) | 88.2 (3) | 89.4 (1) | 90.8 (2) |
| X(2)–Mo–P(1) | 173.50 (6) | 167.0 (4) | 161.7 (4) | 162.4 (1) | 167.5 (2) |
| X(2)–Mo–P(2) | 80.81 (6) | 84.5 (3) | 84.1 (3) | 86.2 (1) | 84.6 (2) |
| X(2)–Mo–P(3) | 86.73 (6) | 82.6 (3) | 84.6 (3) | 85.0 (1) | 85.0 (2) |
| P(1)–Mo–P(2) | 95.75 (6) | 94.0 (1) | 93.8 (1) | 94.4 (1) | 98.2 (2) |
| P(1)–Mo–P(3) | 95.22 (5) | 98.1 (1) | 97.5 (1) | 93.8 (1) | 92.4 (2) |
| P(2)–Mo–P(3) | 161.43 (5) | 166.8 (1) | 168.6 (1) | 171.2 (1) | 169.4 (2) |

[a] Numbers in parentheses are estimated standard deviations in the least significant digits. [b] This work. [c] Reference 2.

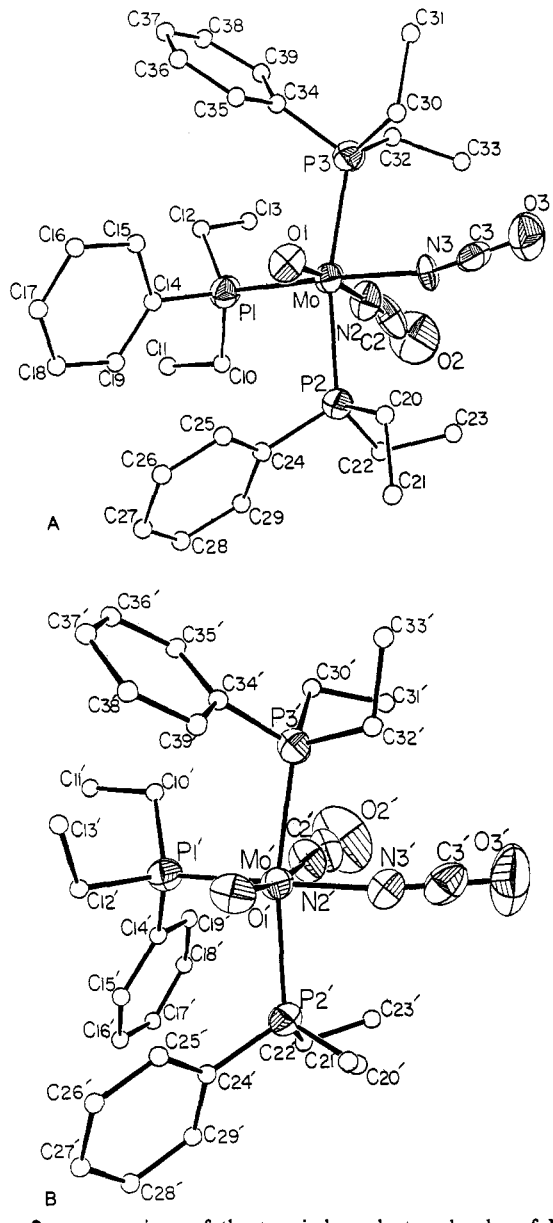


**Figure 2.** ORTEP views of the two independent molecules of $MoO(NCO)_2(PEt_2Ph)_3$ (**2**): (A) molecule **2a**; (B) molecule **2b**. Carbon atoms on the phosphine ligands are shown with arbitrarily small displacement parameters for the sake of clarity.

on the same side of this plane as the oxygen atom, and the methyl group lies on the same side of the plane as the chlorine atom that is trans to the oxygen (see Figure 1). By orienting in this manner, the phosphine ligands can efficiently fill space about the molybdenum with a minimum of steric contacts. All three metal to phosphorous bonds are quite close in length. The Mo—$Cl_{cis\text{-}to\text{-}O}$ bond is ca. 0.05 Å shorter than the Mo—$Cl_{trans\text{-}to\text{-}O}$ bond, and the Mo=O distance is 1.669 Å.

Compound **2** also has a cis-mer configuration of ligands. Two independent molecules, **2a** and **2b**, are present. The coordination about the central metal atom in these molecules is the same, but the orientation of the organic groups on the phosphine ligands differ. In **2a** (Figure 2A) there is a virtual mirror plane coincident with the plane defined by the molybdenum, oxygen, both nitrogens, and one phosphorous atom. This orientation of ligands is virtually identical with that in the blue isomer of $MoOCl_2(PMe_2Ph)_3$.[2b] In **2b** (Figure 2B) the phosphine ligand trans to a cyanate ligand has an orientation different from that in **2a**. The two orientations are related by a rotation of ca. 120° along the Mo–P axis. Because of this different orientation, molecule **2b** has no virtual symmetry. This difference in orientation of the organic groups on the phosphine ligand results in different steric requirements for the ligands, and while the M–L bond distances are nearly the same in the two molecules, some of the L–M–L angles are significantly different. In each molecule the Mo–O distance is short (≈1.68 Å) and the Mo–$N_{cis\text{-}to\text{-}O}$ bond is about 0.08 Å shorter than the Mo–$N_{trans\text{-}to\text{-}O}$ bond.

## Discussion

Distortional isomerism is a rather rare and poorly understood phenomenon. We wish to emphasize that it is fundamentally different from ordinary steric distortions, crystal packing effects, or so-called "polymorphism". Distortional isomerism is not a solid-state effect. Metal to terminal oxygen bonds are quite strong, and it is unlikely that simple packing forces would be enough to distort these bonds to the extent seen (>0.1 Å). Crystals of the two isomers of $WOCl_2L'^+$ are isomorphous, and the crystal packing forces in these compounds would be expected to be similar. In cases where isomers of two different colors can be isolated in the solid state, they are also isolable in solution. Often in solution one isomer is more stable than the other, and interconversion between the two can be seen. While the infrared and electronic spectra of distortional isomers are qualitatively similar, specific absorptions do change appreciably.

The first $MoOX_2L_3$ complex that we structurally characterized was $MoOCl_2(PMePh_2)_3$. When the Mo=O and Mo—$Cl_{trans\text{-}to\text{-}O}$ distances in **1** are compared with those in other $MoOX_2L_3$ compounds, it is clear that green $MoOCl_2(PMePh_2)_3$ more closely resembles the blue isomer of $MoOCl_2(PMe_2Ph)_3$ and blue $MoO(NCO)_2(PEt_2Ph)_3$ than green $MoOCl_2(PEt_2Ph)_3$. To date the green compounds studied have always had longer M–O bonds and the blue compounds have always had shorter M–O bonds. The existence of a green $MoOX_2L_3$ complex with a relatively short Mo=O and long Mo—$X_{trans\text{-}to\text{-}O}$ bond raises the possibility that distortional isomerism in these complexes might be more widespread than originally thought. A hypothetical distortional isomer of the $MoOCl_2(PMePh_2)_3$ complex described would surely have a longer Mo=O bond (≈1.8 Å), yet since the trend is toward greener color as the Mo=O bond is lengthened, it should be green in color, too. Since the two isomers could not be distinguished by color, the existence of a second isomer of $MoOCl_2(PMePh_2)_3$ would go undetected during normal lab work.

A survey of known $MoOX_2L_3$ compounds[1] shows the blue complexes all have more basic X and L groups (e.g. X = $NCS^-$, $NCO^-$; L = $PMe_2Ph$, $PEt_2Ph$) while the green complexes have less basic X and L ligands (X = $Cl^-$, $I^-$; L = $PMePh_2$, $PEtPh_2$, etc.). The two compounds for which both green and blue isomers exist have a combination of a more basic L group and a less basic X group (e.g. X = $Cl^-$; L = $PMe_3$, $PMe_2Ph$). Evidently the color of these complexes is fairly sensitive not only to the Mo=O distance but also to the basicity of the other ligands, and to date isomers of different colors have only been seen in cases of borderline ligand basicity.

Knowing that the color of these complexes is dependent on not only the Mo–O distance but also on the other ligands present and already having one violation of the color/bond distance trend (a green compound with a short Mo–O bond), we wondered whether a blue compound might exist with a long Mo–O bond. $MoO(NCO)_2(PEt_2Ph)_3$ seemed to be a good candidate as it has a $\nu$(Mo–O) of 940 $cm^{-1}$, which is of lower energy than $\nu$(Mo–O) for other blue $MoOX_2L_3$ compounds and in the same energy range as $\nu$(Mo–O) for the green compounds.[1] However, we were disappointed to find that in the crystals we grew of **2** the Mo–O bond is short (≈1.68 Å). Two conclusions can be drawn from this crystal structure. First, that the $\nu$(Mo–O) values, like the colors of these compounds, are sensitive not only to the Mo–O distance but also to the ligand set involved. While the trend is for complexes with short Mo–O distances to have higher energy stretches, $MoO(NCO)_2(PEt_2Ph)_3$ has a short bond but also has a relatively low energy stretch. Second, since this compound crystallized with two slightly different molecules per asymmetric unit, we can draw the following conclusion. In his study Chatt found many differences between blue $MoOCl_2(PMe_2Ph)_3$ and green $MoOCl_2(PEt_2Ph)_3$. We believe these differences may be divided into two types:

A. The first type includes those differences that are caused by the different steric and electronic requirements of the ligands. These would include differences in L-Mo-L bond angles and slight differrences in Mo-L bond distances.

B. The second type includes those differences that are the manifestation of distortional isomerism. On the basis of Weighardt's study of distortional isomers of $WOCl_2L^+$, these differences are limited mainly to the M-O and $M-L_{trans\text{-}to\text{-}O}$ distances. From our study of $MoO(NCO)_2(PEt_2Ph)_3$, we conclude that changes in the orientation of the organic groups on the phosphine ligands may cause minor changes in some bond distances and angles (like those described in A above) but that these changes do not necessarily lead to distortional isomers. Although we did not find a blue $MoOX_2L_3$ molecule with a short Mo-O distance in this case, we still feel that such a molecule might exist.

## Conclusion

The cocrystallization of two conformers of blue $MoO(NCO)_2(PEt_2Ph)_3$, which differ in the arrangement of the organic groups about the phosphorous atoms but not in Mo-O distance, complements Wieghardt's findings that the difference between distortional isomers of $MOL_5''$ compounds lies in different M-O and $M-L_{trans\text{-}to\text{-}O}$ distances and not in the orientation of the ligands. The structure of $MoOCl_2(PMePh_2)_3$ is noteworthy as it is a green $MoOX_2L_3$ compound with a short Mo=O bond. Distortional isomerism in $MOL_5''$ systems has previously been seen only in the few cases that isomers of different colors (blue and green) have been observed. While we present no direct evidence for other complexes for which two isomers exist, our finding of a short Mo=O bond in a green $MoOX_2L_3$ complex suggests that distortional isomerism in these compounds might not be limited to cases in which isomers of different colors are observed. However, whether distortional isomers of these compounds can be prepared and identified as such remains to be seen.

**Acknowledgment.** We are grateful to the Robert A. Welch Foundation (Grant No. A-494) for financial support. M.P.D. is a National Science Foundation Predoctoral Fellow and also holds a Texaco/IUCCP Fellowship from this department.

**Registry No.** **1**, 109362-28-9; **2**, 109428-74-2.

**Supplementary Material Available:** Tables of anisotropic displacement parameters, complete bond distances and angles, and final atomic positional and isotropic equivalent displacement parameters for the nonessential carbon atoms on the phenyl rings for both structure determinations (12 pages); listings of observed and calculated structure factors (37 pages). Ordering information is given on any current masthead page.

---

Contribution from the Department of Chemistry, Georgetown University, Washington, D.C. 20057

# Bonding and Electronic Structure of Conducting Mercury Networks: $KHgC_{4n}$ Graphite Amalgams and $Hg_3MF_6$ Layers and Chains

Miklos Kertesz*† and Arnold M. Guloy

*Received February 4, 1987*

Linear chains, close-packed layers, and honeycomb networks of Hg are found in several highly conducting materials. For positively charged Hg systems it is the layers and chains that are calculated to be more stable, whereas for negatively charged ones it is the honeycomb network that is found to be more stable, in agreement with experiments. The electronic structures of these compounds exhibit high densities of states around the Fermi level explaining some of their unusual properties. The small degree of orbital mixing between graphite and the amalgam layer in the graphite compound on the one hand and between Hg and the anions in the linear-chain and layer compounds on the other hand permits a simple interpretation of the results, which is based on a rigid band model. Bonding in the partially negatively charged honeycomb Hg lattice may be approximately described by $sp^2$ hybridization and in the linear chains by sp hybridization. The breakup of $(Hg^{1/2+})_\infty$ chains into $Hg_4^{2+}$ ions is derived from a Peierls distortion.

The electronic structures of several mercury compounds exhibit unusual properties, such as high electrical conductivity; some are even superconducting. Such is the case for the potassium graphite amalgams[1] $KHgC_4$ and $KHgC_8$. The former is a first-stage and the latter a second-stage Graphite Intercalation Compound, GIC.

The first-stage potassium amalgam GIC, $KHgC_4$, consists of alternating layers of carbon (A, B, ...), potassium ($\alpha$, $\beta$, ...), and mercury (a, b, ...) whose layer stacking sequence is

$$A\alpha a\alpha A\beta b\beta A\gamma c\gamma A\delta d\delta A$$

Hg atoms occupy prismatic sites between potassium atoms as shown in Figure 1, which form a three-coordinated, almost planar, honeycomb network. The projected view of the crystal structure on the *a-b* plane is shown in Figure 1b.

The second-stage potassium amalgam GIC, $KHgC_8$, also has the same two-dimensional structure along the *a-b* plane but differs in the stacking sequence.

In this paper we discuss the electronic structure and bonding of these compounds together with the infinite-chain compounds $Hg_{3-\delta}MF_6$ (M = As, Sb, Nb, and Ta)[2,3] as well as the compounds $Hg_3NbF_6$ and $Hg_3TaF_6$.[2,4] The last two solids have close-packed Hg layers. What makes this structural diversity remarkable is that the formal electron count ranges from ~-0.5e in the graphite compounds to $\sim+^1/_3$e for the chain and layered compounds. The infinite-chain systems consist of incommensurate Hg chains in-

**Table I.** Summary of Calculations on $KHgC_{4n}$ ($n$ = 1, 2)

| syst | Fermi level, eV | $\Delta E$,[a] eV | charge, e | |
|---|---|---|---|---|
| | | | Hg | C |
| $KHgC_4$ ("ideal")[b] | -9.77 | 0.213 | -0.873 | -0.020 |
| $KHgC_4$ ("buckled")[b] | -9.76 | | -0.860 | -0.020 |
| $KHgC_8$ ("ideal") | -9.95 | 0.209 | -0.824 | -0.016 |
| $KHgC_8$ ("buckled") | -9.87 | | -0.781 | -0.020 |

[a] $\Delta E = E_{tot}/Hg$("ideal") - $E_{tot}/Hg$("buckled"). [b] "Buckled" refers to the actual buckled structure of the Hg network in the $KHgC_{4n}$ group ($\delta$ = 0.5 Å), whereas "ideal" refers to the planar, $\delta$ = 0 structure.

† Camille and Henry Dreyfus Teacher-Scholar (1984-1989).

(1) (a) Lagrange, P.; El Markini, M.; Guerard, D.; Herold, A. *Synth. Met.* **1980**, *2*, 191. (b) Herold, A.; Billaud, D.; Guerard, G.; Lagrange, P.; El Markini, M. *Physica B+C* **1981**, *105BB+C*, 253. (c) Alexander, M. G.; Goshorn, D. P.; Guerard, D.; Lagrange, P.; El Markini, M.; Ohn, D. G. *Synth. Met.* **1980**, *2*, 203. (d) Iye, Y. *Mater. Res. Soc. Symp. Proc.* **1983**, *20*, 185 and references therein. (e) Timp, G.; Elman, B. S.; Dresselhaus, M. S.; Tedrow, P. *Mater. Res. Soc. Symp. Proc.* **1983**, *20*, 201 and references therein. (f) Delong, L. E.; Yeh, V.; Eklund, P. C. *Solid State Commun.* **1982**, *44*, 1145.

(2) (a) Brown, I. D.; Cutforth, B. D.; Davies, C. G.; Gillespie, R. J.; Ireland, P. R.; Vekris, J. E. *Can. J. Chem.* **1974**, *791*, 51. (b) Schultz, A. J.; Williams, J. M.; Miro, N. D.; MacDiarmid, A. G.; Heeger, A. J. *Inorg. Chem.* **1974**, *17*, 646.

0020-1669/87/1326-2852$01.50/0 